



LIGO Laboratory / LIGO Scientific Collaboration

LIGO-T060021-01-D

Advanced LIGO

26 Dec 2006

Response to Findings from the
HAM-SAS LASTI Experiment/Prototype Review

Riccardo DeSalvo, Dennis Coyne for the HAM-SAS Team

Distribution of this document:
Advanced LIGO Seismic Group

This is an internal working note
of the LIGO Project.

California Institute of Technology
LIGO Project – MS 18-34
1200 E. California Blvd.
Pasadena, CA 91125
Phone (626) 395-2129
Fax (626) 304-9834
E-mail: info@ligo.caltech.edu

Massachusetts Institute of Technology
LIGO Project – NW17-161
175 Albany St
Cambridge, MA 02139
Phone (617) 253-4824
Fax (617) 253-7014
E-mail: info@ligo.mit.edu

LIGO Hanford Observatory
P.O. Box 1970
Mail Stop S9-02
Richland WA 99352
Phone 509-372-8106
Fax 509-372-8137

LIGO Livingston Observatory
P.O. Box 940
Livingston, LA 70754
Phone 225-686-3100
Fax 225-686-7189

<http://www.ligo.caltech.edu/>

Change Record:

Revision –00: 1/26/2006. preliminary release for comment

Revision –01:1/27/2006. Revised damping to reflect frequency dependence and used measured GAS spring lateral mode Q in the passive isolation prediction. Added comments on potential for up-conversion from cabling.

1 Introduction

The findings of the review committee for the proposed HAM-SAS experiment/prototype at LASTI are documented in [M060004-00](#). This document provides a response to the review committee's findings.

2 Reference Documents

[M060004-00](#) Review Report for HAM-SAS LASTI experiment prototype proposal

[T060020-00](#) HAM-SAS System Dynamics Model¹

[T060002-00](#) SAS Installation and Tuning Procedure

[G050485-00](#) Inverted Pendulum Studies for Seismic Attenuation

[T970236-00](#) HAM Optics Table Mechanical Design and Analysis

[T010074-03](#) The LIGO Observatory Environment

[P030049-00](#) Low Frequency Seismic Isolation for Gravitational Wave Detectors

[E990303-03](#) Seismic Isolation Subsystem Design Requirements

[E060008-00](#) Tentative HAM SAS internal cabling list and connections scheme

Peterson, J., Observation and modeling of seismic background noise, U.S. Geol. Surv. Tech. Rept., 93-322, 1-95, 1993.

3 Responses

3.1 Response to Finding 2, modeling.

A three-dimensional, multi-degree of freedom, dynamics model of the HAM-SAS system has been developed to aid in evaluating the HAM-SAS design and to help in developing servo-controls ([T060020-00](#)). Control system modeling, based on this dynamics model, is in progress. Further refinements in the modeling are planned during the fabrication and test & evaluation phases of the proposed prototype development.

The current HAM-SAS plant modeling includes:

¹ The passive isolation performance presented in this document is based on the model described T060020-00 with the following exceptions: (1) hysteretic (i.e. structural damping) is approximated in this document, whereas equivalent viscous damping was used in the generation of the transfer functions in T060020-00, (2) a measurement of the Q associated with GAS spring non-vertical modes is used here. These corrections as well as others associated with the Inverted Pendulum elastic modes will be incorporated into T060020-01.

- IP flexures (top and bottom) modeled with beam elements
- IP tube modeled with beam elements
- The Spring-Box structure is modeled as a lumped mass (with moment of inertia matrix calculated from a CAD solid model).
- The Optics Table structure is modeled as a lumped mass (with moment of inertia matrix calculated from a CAD solid model).
- Each GAS Filter spring (32 total) is modeled as identical 6 degree-of-freedom springs, with the vertical spring stiffness tuned for ~ 50 mHz vertical frequency. The stiffnesses of the blades in the other directions are calculated from small perturbations about the tuned, large deflection working point, calculated by a nonlinear finite element solution. The horizontal plane stiffnesses of the Gas Filter blade springs (transverse and longitudinal) were measured and found to be roughly close to the calculated values. (Using the measured values shifts two associated modes from 1.2 to 1.1 Hz)
- The position of all actuators and sensors are represented by nodes with rigid links to their associated lumped center-of-mass (either the Spring Box or the Optics Table).
- The position of a number of cardinal payload points are represented by nodes with rigid links to the optics table lumped mass (center of mass), most notably the suspension point of a triple suspension at it's maximum offset from the table center.
- The quasi-kinematic mounting arrangement between the Optics Table and the GAS filter centers (4 contact points) are constrained in the model to follow the translations of the GAS filter centers; The rotational degrees of freedom are not constrained. This seems appropriate for small motion (friction dominated) dynamics.
- Frequency dependent damping² based on measurements of the loss (ring down) in the 3-legged HAM IP at Caltech. See also the discussion below on damping.
- “Parasitic” springs (4 with 10 N/m each) between the Spring Box and Optics Table in parallel with the GAS Filter vertical spring stiffness. The vertical resonances of the GAS Filters were tuned with these springs already in place. These springs represent vertical tuning/adjustment springs for the GAS Filters and the stiffness of electrical cabling between the Spring Box and Optics Table stages. (See also section 3.4.)

The following aspects are not modeled, or are known to be incorrect:

- The IP counterbalance mass (to set the center of percussion properly) has not been included.
- The IP leg beam cross-section was modeled incorrectly in T060020-00. The first bending resonances appear at 370 Hz in the model, whereas the actual design has resonances at 103 Hz (as measured in the 3-leg HAM IP system at CIT and confirmed by the finite element analysis documented in [G050485-00](#)). These resonances will cause a plateau in the isolation (below the required isolation), which is not present in the current model.

² Note that the transfer functions shown in T060020-00 employ an equivalent viscous damping factor. This will be revised in version -01 to be a more appropriate hysteretic damping model. The results shown in this memo approximate hysteretic damping.

- The structure is only modeled to the base of the IP, i.e. the support structure (support table, support tubes and crossbeams) is not yet included. A dynamics model of the support structure has been developed. (See section 3.5.1 for a heuristic reason why this should not have a significant effect.)
- Structural compliance of the spring-box structure and the optics table. Both of these elements should have first resonances well over 100 Hz and no interaction with the low frequency isolation dynamics. The current plan is to adapt the existing HAM optics table for the LASTI experiment/prototype. The same approach could be used in production. The HAM Optics Table design (D050117), if/when needed (for example to outfit the HAM chambers without tables or with modification to get a larger area), is very similar to the initial LIGO HAM optics table. A finite element analysis of the HAM Optics Table ([T970236-00](#)) indicates a first elastic resonance at 250 Hz.
- The internal modes of the blade springs. The internal modes of the deformed blade spring have been calculated by a finite element analysis, but not included into the overall HAM-SAS system model. The first resonance is at 291 Hz.
- The coupled dynamics/interaction of the HAM-SAS system and suspended/actuated payload elements has not been addressed.
- Eddy current damping for the IP Spring Box and IP resonances (34 to 40 Hz). (See also eddy current damping measurements on a HAM IP in [G050485-00](#).)
- Weak “parasitic” springs in parallel with the IP (cabling and tuning/adjustment springs). (See section 3.4.)
- Perturbations in the geometry or stiffnesses of the HAM-SAS elements, e.g. variations in the GAS spring blade stiffnesses, variation in the IP lengths, etc.

The model has been formulated with the I-DEAS finite element software. A finite element approach was used (as opposed to formulating the dynamical equations in a system like Matlab) in order to minimize development errors (I-DEAS has been extensively verified). However the I-DEAS eigensolver appears to have problems in computing orthogonal modes at the intended ~30 mHz tuned GAS Filter and IP frequencies. Consequently the model was tuned to ~50 mHz for these modes.

The LIGO ground noise spectrum model ([T010074-03](#)) was extended to 10 mHz using the Peterson New Low Noise Model (Figure 1 and cyan curve in Figure 3). A ground tilt noise spectrum model was developed (10 mHz to 40 Hz) using this extended translational spectrum with the approach described in Takamori’s thesis ([P030049-00](#)) (see Figure 2).

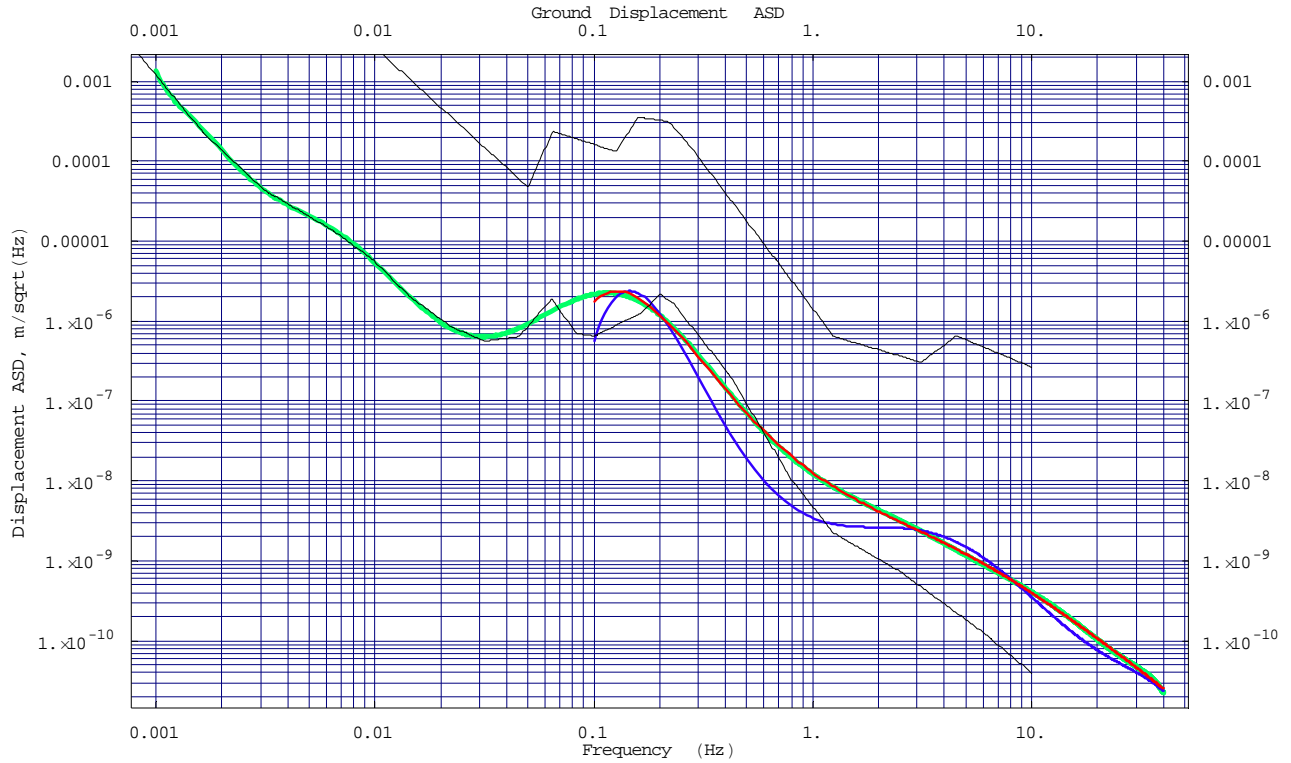


Figure 1: Comparison of the Peterson High & Low Noise Models with the LIGO Models

Peterson's New Low Noise Model (NLNM) and New High Noise Model (NHNM) are shown in the above plot (black lines). A smooth fit (green curve) was made between the NLNM and the LLO ground translational noise model (red curve). The LHO ground noise model is shown also (blue curve).

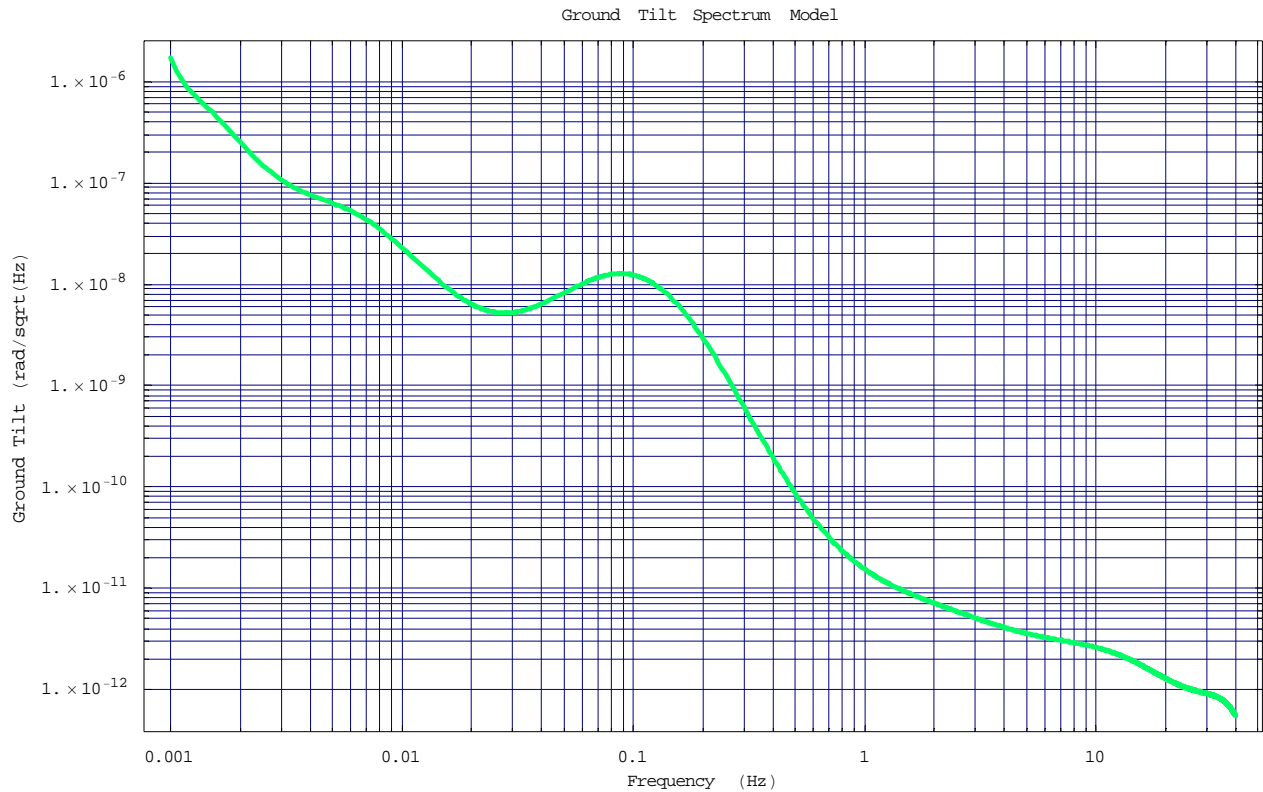


Figure 2: Ground Tilt Noise Model

The base of the HAM-SAS model (the bottoms of the four inverted pendula) were simultaneously excited with the translation PSD (in x, y and z directions) and the rotational PSD (in Rx, RY and Rz degrees of freedom). The result of this random PSD excitation at the suspension point of the triple pendulum mounted on the HAM optics table (at a height of 828 mm above the table and offset from the center of the table by 900 mm) is shown in Figure 1.

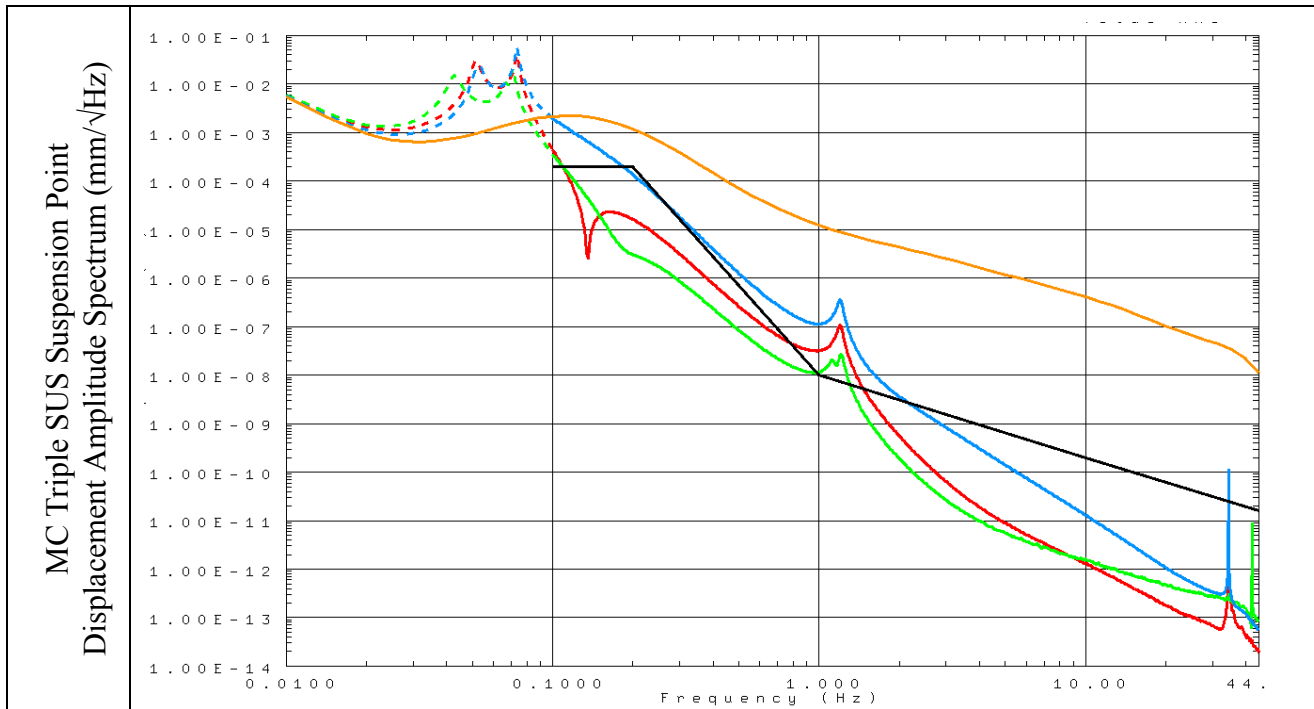


Figure 3: Predicted Passive HAM-SAS Isolation Performance at the Suspension Point of the Triple Suspension

The solid orange curve is an extension of the LLO ground noise model to 10 mHz using the Peterson NLNM. The solid black curve is the isolation requirement from E990303-03. The red, green and blue curves are the x, y and z (vertical) direction translational amplitude spectral density (ASD) in mm/√Hz. The solid curves use a low (equivalent viscous) damping loss factor (0.01%), except for the 3 modes at ~1.2 Hz, where a measured 4.8% loss factor is used. The dashed curves use relatively high loss factors (up to 8.6% equivalent viscous damping) for the 6 lowest modes (43 to 74 mHz) associated with the IP and the GAS Filter. These loss factors are calculated from a fit of loss versus frequency for the HAM-SAS three-leg IP system at Caltech. Our expectation is that the passive performance will follow the dashed curves at low frequency (< ~0.1 Hz) and the solid curves at high frequency (> ~0.1 Hz) with the exception that (a) the isolation will begin to saturate (plateau) at ~10 Hz due to the IP leg modes which are not yet properly modeling and (b) the resonance peaks at ~35 Hz will be eddy current damped.

The model predicts that the isolation requirement (solid black curve in Figure 3 taken from [E990303-03](#)) is met at all frequencies, except from 0.8 to 1.5 Hz³ due to resonances at ~1.2 Hz. These resonances are predicted differential tip, tilt and yaw motions of the optics table and spring box and are a direct result of the predicted (and measured) horizontal plane stiffnesses of the spring blades. The mechanical Q of the lateral mode on a 2-blade GAS filter, with blades similar to the HAM-SAS design, was measured to be 21; this value has been used in the passive performance prediction in Figure 3. The reason for this relatively high measured loss factor, for the maraging steel blade springs, at 1 Hz is not well understood. It is not consistent with the IP maraging flexure loss factor dependence on frequency. Even if the Q was higher, some possibly active and/or passive

³ The vertical direction also exceeds the requirement in the microseismic region (0.1 to 0.3 Hz) and more broadly around the 1.2 Hz region. However, it is noted in E990303-03 that this requirement mostly applies to the test mass isolation systems. Due to the short length between LVEA chambers there should be no relative motion due to the microseismic peak.

(eddy current) damping of these ~ 1.2 Hz modes is feasible without compromising the isolation at 10 Hz.

Measurements of the mechanical damping of the inverted pendulum at resonance⁴ have been made as a function of frequency using the HAM-SAS inverted pendulum legs under their nominal load. These measurements spanned from 1 Hz ($Q=3000$) down to 60 mHz ($Q=11$). From a fit to the data,

$Q(f) = \frac{f^2}{1.6 \cdot 10^{-5}(f^2 + 19.6)}$, the Q at 30 mHz is predicted to be 3. This $Q(f)$ function was used to

calculate the equivalent hysteretic loss factor, $\zeta = \frac{1}{2Q}$, at resonance for each of the modes (with

the exception for resonant frequencies above 30 Hz, the Q was limited to 10,000). The I-DEAS dynamic response calculation uses (equivalent) viscous damping. For the high damping factors of the IP modes, this causes an apparent $1/f$ roll off behavior (dashed curves in Figure 3). Since all previous implementations of inverted pendula show a $1/f^2$ roll off behavior⁵, and since we expect the damping mechanism to be structural (or hysteretic and frequency independent), we expect to see a $1/f^2$ roll off in the HAM-SAS design, as indicated in the solid curves of Figure 3.

Ground tilt does not contribute significantly to translational motion of the suspension point of the triple SUS, i.e. the ground translational motion dominates in calculation of the suspension point motion.

There is some amplification of ground noise just below the microseismic peak (~ 40 mHz to 70 mHz). The already significant passive damping of these modes can be augmented with active damping to reduce the rms motion. The rms motion is 3.2 microns (integrated down to 10 mHz). If the target tuning frequencies of ~ 30 mHz are achieved, then the total rms will be reduced further since (1) the resonance Q decreases with frequency ($Q=3$ at 30 mHz, $Q=16$ at 70 mHz) and (2) the ground motion spectrum has a ‘dip’ at ~ 30 mHz.

3.2 Response to Finding 3, alternative and cheaper solutions to seismically isolate the OMC chambers.

Although there are undoubtedly somewhat cheaper seismic isolation solutions for the OMC, implementing a full size HAM SAS optical bench will provide the maximum in terms of flexibility and expansion potential. In addition, a “cheaper” solution would introduce a different seismic attenuation scheme than will be used in Ad-LIGO, with a non-standardization cost, and it would have to be designed from scratch, which would require time, additional cost and effort, including separate testing and production. This would reduce the possible savings.

Using the proposed SAS solution for OMC would provide a test of a seismic attenuation technique alternative to, and much cheaper than, the present HAM baseline solution. If successful at LASTI, and then implemented in replacement of the baseline solution, HAM-SAS would represent a large

⁴ Yumei Huang and Riccardo DeSalvo, measurements taken January 2006 on the three-legged IP with HAM-SAS legs and flexures.

⁵ For example, the VIRGO inverted pendulum, tuned to ~ 35 mHz, shows a $1/f^2$ roll off in Figure 7.8 of G. Losurdo, Ultra-Low Frequency Inverted Pendulum for the VIRGO Test Mass Suspension, thesis, Scuola Normale Superiore di Pisa, Oct 1998.

savings in both money⁶ (> \$12M) and effort with respect to the present AL baseline. The hardware investment cost for the IL OMC (~3 x \$477K = \$1.4M⁷) would be fully recouped in advanced LIGO.

The suppression of the HEPI pre-attenuation stage, and the replacement of the two in-vacuum, active control stages with a single passive attenuation level with controls which are essentially limited to DC positioning lead to large savings in complexity and control efforts that are difficult to underestimate. The virtual elimination of heat dissipation, and the elimination of pressurized sensors inside the vacuum enclosure bring a reduction of risks that also should not be underestimated.

3.3 Response to Finding 4, complete redesign after satisfaction of point 2?

We do not think that a redesign is needed. See response to point 2 above.

3.4 Response to Finding 5, cabling

Threaded holes have been foreseen at regular intervals around all sides of each platform. These holes are intended to fasten cable clamps that will strain relief cables between each attenuation stage. Different kinds of cable clamps have been foreseen for different geometries. Given the previous LIGO experience, no specific detailed cable routing scheme has been formulated because such routing depends on the specific end use. It is foreseen that ~20 cables⁸ will thread all the way to the top of the optical bench. A 1 to 2 feet long loop is foreseen between each clamping point pair. The cable stiffness measured for a 1 foot long cable, 1 N/m, should be compared with the

⁶ The current estimate for the HAM-SEI baseline (2 stage active system) is \$1087K per chamber in hardware costs (materials, supplies, subcontracts) and \$1351K per chamber total (including LIGO labor). The hardware costs for a single HAM-SAS prototype are \$477K. All estimates are in FY05 \$. So the hardware cost savings should be at least \$610K x 15 chambers = \$9.1M. In addition, if the HAM-SAS system does not need the HEPI pre-isolation, an additional savings of \$291K per chamber (hardware costs only) x 10 LHO chambers = \$2.9M. So the total hardware cost savings could be \$12M. Additional labor cost savings are also expected, but have not been estimated.

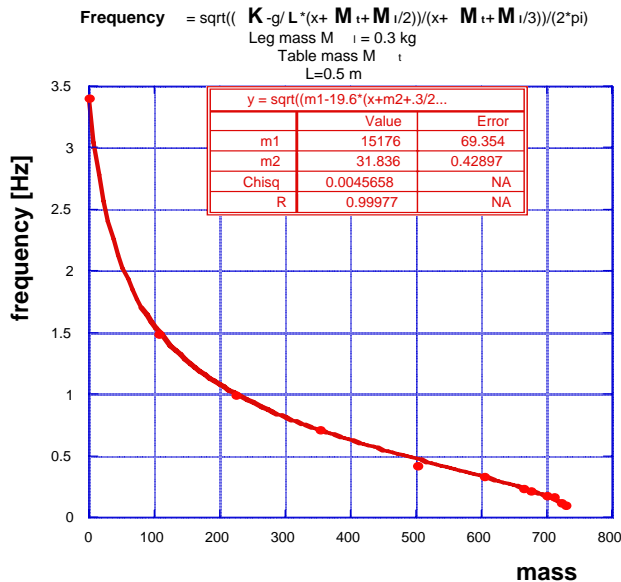
⁷ Not counting in deduction the cost of the “cheaper” solution

⁸ Assume 20 standard cables, each 25 conductor (twisted pair, overall-shielded and with an open weave PEEK jacket to prevent shorting to the shield) to instrument 2 triple pendulums, 2 single pendulums and a suspended photodiode and 10% spare.

5,000 N/m of equivalent stiffness of each single IP leg before stiffness cancellation⁹, and a similar amount for the blades before GAS cancellation. The tuned stiffnesses of the four IPs and the four GAS filters are approximately 32 N/m each. The cable stiffness (~20 N/m total) can be compensated (cancelled) the same way as we routinely compensate for the parasitic tuning spring stiffness by mounting cable sections in parallel to the main springs while tuning the GAS and the IP stiffness. The small differences due to cable-to-cable routing differences are such that they do not represent a concern even in a soft system.

For the internal SAS cabling please see also LIGO document [E060008-00](#). The cables laid across SAS will have suitable strain relief, free length and connector terminations for easy connections to both the feed-through and user end. See also the installation plan report already provided to the committee.

The cable braiding obviously generates some level of up-conversion noise. However, we expect that the cable up-conversion noise will remain below the requirements level. At the optics table stage the up-conversion noise is strongly depressed by the ratio of the large optics table mass and relative weakness of the noise (force) generation in the cables. We can expect that the cables in advanced-LIGO will generate on the optics table no more noise than what is presently detected on the initial-LIGO optical benches downstream of the stacks¹⁰. If we assume that the observed up-conversion bump in IL (at a level of $\sim 10^{-18}$ m/ $\sqrt{\text{Hz}}$) is due to noise generated in either the cabling to the table or the constrained-layer damped springs, then the up-conversion corresponds to an optics table motion of $\sim 10^{-15}$ m/ $\sqrt{\text{Hz}}$ (using ~ 1000 for the isolation of a single pendulum at ~ 30 Hz). This is well below the SEI requirement of 2×10^{-13} m/ $\sqrt{\text{Hz}}$ at 10 Hz. If despite these factors up-conversion proves to be a limiting factor in Virgo¹¹, or later in the advanced-LIGO quadruple



9

The IP linear stiffness (measured in the HAM SAS 3 legged prototype) is $\sim 5,000\text{N/m.leg}$

¹⁰ As a source of noise the cables are potentially much weaker than the initial-LIGO composite springs, which should reduce the problem below the present level.

¹¹ Virgo is more sensitive to up-conversion problems because its cabling runs along the main attenuation chain.

pendulum, we can change to laminated (or other form of non-braided) cables to mitigate the problem.

3.5 Response to Finding 6

3.5.1 Floor compliance:

The IL support structure comprised of the piers, gull-wings (i.e. crossbeams), support tubes and base platform (i.e. support table) has a first resonant frequency above 10 Hz, pretty well decoupled from the ~30 mHz resonant frequency of the IP or GAS filters. There is therefore expected to be marginal couplings between the structure and the SAS.

Also See point 7 and the pending analysis under point 2.

3.5.2 b) Test setup compliance.

The test setups mentioned by the committee (assy. LIGO D051149-50-51 and 56) were intended to perform a pre-LASTI validation of the HAM SAS performance in order to separate possible issues related to the LASTI site from HAM SAS issues. It has been estimated that the measurements of attenuation properties that will be feasible at LASTI will be adequate. The test setups were also intended for the tuning of the counterweights of the IPs and the GAS compensation wands. It was considered that the IP counterweight tuning can be performed equally effectively¹² by means of ANSYS calculations and simple tests of the unloaded leg, without the need of the test setup illustrated in assy. LIGO D051149-50-51, which was therefore suppressed. Similarly the tuning of the wand's counterweight can be done at the filter's level with the simplified setup illustrated in assy. LIGO D051176; the setup of assy. LIGO D051156 was also suppressed.

3.6 Response to Finding 7 Effects of ground tilts.

The floor tilts should be divided into two categories, long term tilt shifts and dynamic tilts like the ones provided by wind or seismic motion.

There is plenty of experience of long term tilts both in Virgo and at LIGO. The ground at the West end station of Virgo has sunk by more than a cm. The effect is mostly vertical, but all residual tilt effect are easily being dealt with the voice coil actuators and parasitic tuning springs. The floor of the Synchrotron hall, where all LIGO tests were performed, tilts North to South in rainy seasons¹³. Even in these extreme conditions, there was no problem to hold in place the 4 m tall, 1 ton payload LIGO IP prototype using the voice coils alone. Of course, in HAM SAS long term tilts would be corrected by means of the parasitic springs to minimize the standing current in the voice coils. It may be useful to consider that tilt of 1 milliradian over the 1 ton payload would require only 10 N of corrective force from the tunable parasitic springs which therefore have plenty of correction strength and range for any conceivable condition. Larger tilts (generated for example by really large earthquakes) would require re-alignment of the scissor tables.

¹² The IP leg balancing is necessary only to push the performance beyond 80 dB; only balancing of the leg to 10% accuracy is necessary.

¹³ Water infiltrations in the North side make the Synchrotron cork layer (1 foot thick, designed to damp vibrations during the grinding of the 200 inch telescope mirror) under the concrete floor to swell on that side

Regarding dynamic tilts, an IP does not distinguish tilt from a horizontal acceleration, it therefore attenuates any tilt motion faster than its resonant frequency, nominally 30 mHz. Note that once an IP is tuned at such low frequency that its Q factor approaches 1 (3 at 30 mHz, 16 at 70 mHz), and there is little amplification even at the resonance. The effects of lower frequency tilts will be corrected in the same way than the very low frequency oscillations, feeding back from the LVDT position sensor (except when and where the LVDT signal is overruled by the global interferometer length signal). See the analysis under the response to finding 2 for more regarding tilt to horizontal coupling.

3.7 Response to Finding 8 Altering payload.

Just as for initial LIGO, the intent is to have an invariant payload total mass, with the payload center of mass (C.M.) adjusted to be at the table center through the use of stainless steel make-up masses. The payload C.M. will be of varying height above the optics table depending upon the complement of items that comprise a particular table's payload. In general it should not be necessary to re-tune the SAS when payload items (and counter-weights) are adjusted. However, if needed, one can re-tune the SAS, as described in installation plan report T060002-00-E.

It may be of interest to note that HAM SAS is designed modularly. The payload can be substantially reduced (or increased) by changing the number and width of the GAS blades and diameter of the IP flex joints. Optical benches that are known that will have much smaller optical payload (for example the OMC benches) could be equipped with these lightened HAM SAS if there was perceived advantage in doing so. Similarly, higher than HAM design payloads could be accommodated in the same way.

3.8 Response to Finding 9, Installation and fixturing plan

See installation plan report T060002-00.

3.9 Response to Finding 10, Drift measurements

Both IP and GAS filters are kept in place by DC feedback. This means that the position stability is essentially just as good as the stability of the electronics of the position sensors and their supporting structures.

Note that very low frequency feedback from beam length sensing would make the drift irrelevant in the beam-line direction. The HAM-SAS team will work with the LASTI group to develop an experimental plan to monitor the drift with instrumentation independent from the feedback sensors.

3.10 Response to Finding 11, Performance and Experience of TAMA and VIRGO systems

Unfortunately there is little recently published data¹⁴ from either Virgo or TAMA. The SAS team is aware of this shortcoming, which is balanced by the fact that we had uninterrupted, tight collaboration and/or extensive interactions with both Virgo and TAMA. These interactions ensured that all the information was available for the design of the SAS for LIGO and that the lessons learned from Virgo and TAMA were properly incorporated in the proposed design. The best people working in Virgo and TAMA actually assisted us with their advice, review and criticism in the LIGO SAS concept and design. Riccardo DeSalvo and Virginio Sannibale participated in the design, prototyping and early construction of the Virgo Superattenuators. R.D.S., V.S. and Szabi Marka have collaborated to the deepest level with Akiteru Takamori and the TAMA team to develop the TAMA SAS prototypes (which were developed, designed and assembled in Caltech) and their successful testing in the 3 m experiment, as well as its ongoing installation in the TAMA interferometer itself. Even in absence of complete documentation from either Virgo and TAMA, we believe that the SAS team staff have proper and sufficient know-how to insure the best possible use of SAS for LIGO's benefit due to the extensive Virgo & TAMA experience.

After recent consultations with our Virgo and TAMA peers the following list of the main lessons learned and applied to the design of the SAS for LIGO was compiled.

It has to be stressed first that the LIGO SAS (or equivalently the present baseline LIGO active seismic attenuation system) have to be compared only with the IP and Filter Zero pre-attenuators of Virgo or TAMA. The comparison should not extend to the complete attenuation chains, which for Ad-LIGO would comprise also the underlying triple and quadruple pendula. Most of the problems that have been encountered in Virgo and/or TAMA are not relevant in the LIGO optical bench case.

Lesson 1 (Virgo)

The Virgo IP performance has been limited by the low resonant frequency (9 Hz) of its legs. In the SAS for LIGO this resonance was moved up by more than an order of magnitude.

¹⁴ Losurdo suggest that the following two publications might have escaped from the committee attention.

[16] G.Losurdo, et al.: "An inverted pendulum preisolator stage for the VIRGO suspension system", *Rev. Sci. Instrum.*, **70** (5), 2507-2515, 1999.

[22] G.Ballardin, et al., "Measurement of the VIRGO superattenuator performance for seismic noise suppression", *Rev. Sci. Instrum.*, **72** (9), 3643-3652, 2001.

[23] G.Losurdo, et al., "Inertial control of the mirror suspensions of the VIRGO interferometer for gravitational wave detection", *Rev. Sci. Instrum.*, **72** (9), 3653-3661, 2001.

[33] S.Braccini,..., G.Losurdo, ..., *et al.* (the VIRGO Collaboration), "Measurement of the seismic attenuation performance of the Virgo Superattenuator", *Astrop. Phys.*, **23**, 557-565 (2005).

[P8] G.Losurdo for the VIRGO Collaboration, "The inertial damping of the VIRGO Superattenuator and the residual motion of the mirror", *Proc. of the Fourth E.Amaldi Conference on Gravitational Waves*, Perth, Australia, 8-13 July 2001, *Class. Quantum Grav.*, **19**, 1631-1637, 2002.

Lesson 2 (Virgo)

There have been limitations on the Virgo IP performance due to the cradle effect (a horizontal accelerometer mounted on a swing cannot properly detect the oscillation of the swing due to the equivalence principle, i.e. cannot distinguish between tilt and horizontal motion). This deficiency made it difficult to lower the cross-over frequency between the position and the accelerometer signal in the feedback. This problem was mitigated in Virgo by using the position sensor information to correct the accelerometer signal (The IP leg rigidity ensures that the cradle motion happens in a well defined surface and the accelerometer tilt is precisely predicted by the IP position in the horizontal plane). All Virgo towers are now equipped with this correction and are tuned to 30 mHz resonant frequency (down from 70 mHz with a tenfold improvement of seismic noise re-injection). It is expected that at the next startup Virgo will profit from this improvement.

In LIGO this problem can be cured at the outset by improving the IP leg alignment to better than a few parts in ten-thousand precision and thus greatly reducing the cradle effect (this step was not correctly implemented in Virgo) [see assy. Procedure, T060002, and D051148]. Any residual effect will be corrected “a la Virgo” using the SAS LVDT signals.

Lesson 3 (Virgo)

Below the correction for the cradle effect, there is a suspected wind induced ground tilt effect. This effect is believed to be particularly bad in Virgo (much worse than in LIGO) because of facility limitations. The Virgo building stands out above an artificial hill, it is tall and narrow, built to be extremely rigid, and is directly connected to the Virgo concrete platform. Wind pressure results in a comparatively large floor tilting torque. In LIGO the building aspect ratio is much more favorable (the building is much lower and wider) and the building is supported by a separate foundation. Also the HAM SAS legs are one order of magnitude shorter than the Virgo ones. Much less wind related tilt can be expected in LIGO. Therefore the ground tilt problem, already not critical in Virgo, should be of much less concern in LIGO.

Note also that the lowest frequency drifts induced by tilt are cancelled by DC controls based on the LVDT position sensor signals or, when available, on the global control beam length signal itself.

Lesson 4 (Virgo)

Virgo suffers from a lack of low frequency vertical pre-isolation. It's Filter Zero has been tuned at the standard 300 mHz and lacks the capacity of being tuned down to 30 mHz to match the IP tuning¹⁵. Realizing this shortcoming was one of the drivers in developing M. Mantovani's e.m. springs, an important development which is implemented in the LIGO GAS filter design.

Lesson 5 (Virgo)

Already in the initial Virgo installation it was clear that the magnetic anti springs were strongly temperature sensitive. The GAS spring development, whose thermal frequency dependence is so much less to be hardly measurable, answered to half of that lesson. The second half, the natural and unavoidable strong thermal movement of the filter's working point when the return forces are

¹⁵ The special Filter Zero described in the following reference was tested but never implemented in Virgo. R.De Salvo, et al.: “Performances of an ultralow frequency vertical pre-isolator for the VIRGO seismic attenuation chains”, *Nucl. Instr. and Meth. in Phys.Res. A*, **420**, 316-335, 1999.

depressed by the Geometrical Anti Spring mechanism, was addressed by the implementation of the temperature correction also developed by M.Mantovani and implemented in the LIGO SAS. This implementation means that the thermal blanket feedback, used in Virgo to stabilize the superattenuators, is not necessary in the LIGO SAS.

Other lessons (Virgo)

Finally Mattt Evans, who had the occasion to work both on LIGO and Virgo was interviewed, he was asked which features would he advice for our HAM SAS, the HAM SAS design was reviewed and the list of his suggestions were checked again.

He basically advocated that all degrees of freedom be properly damped and that suitable sensors and actuators be implemented in all degree of freedom. All his suggestions were deemed already properly taken care of in the present HAM SAS design.

He also added the following requirement: "Knowing what little I do about suspensions, I would say that in addition to the noise requirement, I would require that the active system be capable of a "virtual lock-down" in which the platform is locked to the position sensors with a bandwidth of about 10Hz. The noise of such a state (as seen by a witness on the table) should be dominated by the ground motion spectrum up to 100Hz, the actuator should assume a servo cut-off at about 100Hz (10 times the UGF) and should have some headroom (a factor of 10 more range than sensor/seismic noise at all frequencies). A quick calculation shows that for 100kg payload, and 10nm/ $\sqrt{\text{Hz}}$ at 10Hz, the actuator should have about 100mN of range up to 100Hz."

This final requirement is satisfied by the actuators (a typical actuator authority is 1 N/A, which is more than necessary even for the larger HAM SAS payload. The actuator authority can be reduced by one or more of the following three methods: reducing the strength of the permanent magnets, reducing the number-of-turn density in the actuator coils and reducing the current in the coils by means of suitable external resistors) even for a full 1 ton payload.

Lessons (TAMA)

The TAMA SAS design is very close to the SAS for LIGO. Therefore, more than from lessons learned, LIGO is directly profiting from the TAMA SAS experience.

As examples:

The HAM GAS filters use the identical blades as the TAMA GAS filters (except for the COP correction wand that has been developed later).

Sensors and actuators are essentially the same developed for TAMA SAS.

Some of the testing equipment developed for the TAMA IP was used to test the LIGO SAS IP legs.

All tests and development performed for TAMA have been directly applied to the LIGO SAS design and some in the quadruple pendulum design.

Members of the review panel made some comment about the failure of the TAMA 3 m experiment to prove that TAMA SAS reached its simulated performance. Part of the discrepancy was attributed by the experimenters to deficiencies of the measurement setup. Akiteru, during his thesis

work, did not have the means and the time to upgrade the experiment and ‘fine-tune’ the simulation to discriminate between the deficiencies of the setup and deficiencies of the system. But, the most important features for TAMA, the large improvement of seismic noise below several Hz and the stable operation of the suspended Fabry-Perot cavity were successfully demonstrated. If the panel is overly concerned with the discrepancy between the original simulation and the experiment, it may be useful to consider that, although little written account (in English) was made of the TAMA SAS development beyond Akiteru Takamori’s thesis, all the available information was carefully and independently vetted by the TAMA scientists ‘to satisfy the tight requirements which are at least comparable to those of the pre-attenuation requirements required from the LIGO SAS or from the active SEI’. As a consequence of that vetting process the SAS technique was adopted for the seismic attenuation and mirror suspensions of both TAMA¹⁶ and LCGT.

Members of the review panel should feel free to contact Giovanni Losurdo, Lee Holloway and/or Diego Passuello at Virgo and Akiteru Takamori and/or Ryutaro Takahashi at TAMA, which are between the most expert cognizant scientists in this field. They all apologize for the lack of information provided, and will be happy to try answer any question from review panel members.

3.11 Finding 12: Schedule, Labor and Plan.

The proposed schedule and skilled manpower requirements for the procurement, fabrication and test programs should be identified explicitly.

To be done.

¹⁶ For curiosity, the following are the last news (January 12th) from the installation of TAMA in SAS. Unfortunately they do not give much detail relevant for the HAM design: “I inform you about the present status of the TAMA-SAS at NAO. The first SAS-tower was installed to the EMI chamber in September, 2005. We found that the natural horizontal frequencies of IP were 46mHz and 154mHz. The rotational (Yaw) frequency of IP was 0.54Hz. The fundamental frequency of GASFs was 0.48Hz. The digital controller using commercial systems is successfully working to damp these mechanical modes. Still we are adjusting the SAS-tower to work in the interferometer. I expect the performance of the first SAS is partially confirmed by the interferometer by February. I want to install the next SAS towers for the NMI chamber to construct one arm by April. All of towers will be completed in summer, 2006. Ryu”